

Color Halftoning with Generalized Error diffusion

Daniel L. Lau

Department of Electrical and Computer Engineering
University of Delaware
Newark, DE 19716, USA
lau@ece.udel.edu

Abstract

In this paper, we introduce a novel technique for digital color halftoning with green-noise, stochastic dither patterns composed of homogeneously distributed minority pixel clusters. This new technique employs scalar error diffusion with output-dependent feedback in each of the four process colors where, unlike mono-chrome halftoning, an interference term is added such that the overlapping of pixels of different colors can be regulated for increased color control. As is the case with monochrome halftoning, this new technique is tunable, allowing for large clusters in printers with high dot-gain characteristics and small clusters in printers with low dot-gain characteristics. This new technique also incorporates several other advancements that have been introduced since error diffusion's original inception including edge enhancement through threshold modulation.

1. Introduction

In digital printers, amplitude modulated (AM) halftoning is done through clustered-dot ordered dither where the original continuous-tone image is divided into sub-blocks which are then thresholded pixel-by-pixel with a dither array composed of consecutive thresholds clustered together. The ultimate goal of halftoning is to produce the illusion of continuous-tone without the viewer seeing the black and white dots. So a real problem with clustering consecutive thresholds is that it produces large macro-dots that are clearly visible to the viewer, or at least more visible than if consecutive thresholds are isolated as much as possible as in the case of Bayer's dither. The problem with Bayer's dither is that the thresholds form a regular pattern of dots, something that the viewer's eye is very sensitive to and therefore clearly sees as an artificial texture [1]. This patterning is also a problem for AM algorithms being composed of a *regular* grid of dots.

In 1976, Floyd and Steinberg [2] came up with a solution for the problems associated with Bayer's dither when they introduced error diffusion – an adaptive algorithm that quantizes each pixel, one-at-a-time, passing on the quantization error to neighboring, unprocessed input pixels. Error diffusion's real benefit is that it not only isolates printed pixels, but it also does so in a random fashion, creating dither patterns composed exclusively of high frequency spectral components.

Ulichney [3] describes these patterns as *blue-noise* where for a given gray-level g , the ideal pattern separates the minority pixels by an average distance of λ_g , the blue-noise *principle wavelength*, such that

$$\lambda_b = \begin{cases} D/\sqrt{g} & , \text{ for } 0 < g \leq 1/2 \\ D/\sqrt{1-g} & , \text{ for } 1/2 < g \leq 1 \end{cases} \quad (1)$$

where D is the minimum distance between addressable points on the display. The resulting power spectrum of

these patterns then have spectral components with frequencies greater than or equal to $f_b = \lambda_b^{-1}$, the blue-noise *principle frequency*.

Based on the sensitivity of the human visual system (HVS) to low-frequency graininess, error diffusion creates halftone patterns far superior to AM halftoning or Bayer's dither, exhibiting much higher spatial detail without adding perceptually disturbing or artificial textures. Error diffusion's success at halftoning has since sparked many improvements over its original inception. In 1992, Levien [4] introduced such an improvement when he introduced error diffusion with output-dependent feedback where the quantization threshold is modulated by a linear sum of neighboring output pixels.

By employing this feedback term, Levien demonstrated the ability to vary the coarseness of resulting dither patterns that were now composed of minority pixel clusters. These patterns are described by Lau *et al* [5] as *green-noise* being composed exclusively of mid-frequency only spectral components. Similar to Ulichney's work with blue-noise, Lau *et al* show that for a given gray level g and an average cluster size of M minority pixels, the average separation of clusters (centroid-to-centroid) is λ_g , the green-noise principle wavelength, such that $\lambda_g = M^{1/2} \lambda_b$. The resulting power spectrum of these patterns then have a power spectrum composed exclusively of mid-frequency spectral components with frequencies at or near $f_g = \lambda_b^{-1}$, the green-noise principle frequency.

While the clustered dots of these green-noise patterns are much easier to see than their blue-noise counterparts, they are also much easier to print consistently. Laser printers, being so unreliable or unpredictable at printing isolated dots, are unable to produce blue-noise patterns without introducing severe tonal distortion and without introducing an unacceptably high amount of spatial variation in tone [6]. Being tunable to the reliability of the printer to produce isolated dots, green-noise allows a printer to produce stochastic patterns with just enough clustering as to minimize spatial variations in tone by trading dot visibility for halftone robustness.

Today, applying error diffusion to color halftoning is a "hot" topic among researchers [7]. Typically, schemes fall into one of two categories, either scalar where each color is halftoned independently of the others or vector where the halftoning of channels is done in a correlated fashion. In this paper, I make my contribution by introducing *generalized error diffusion*, a new framework for error diffusion that can be either scalar or vector depending on certain parameter constraints; furthermore, this new framework tries to incorporate several innovations first proposed for monochrome error diffusion such as threshold modulation and output-dependent feedback. Not without novel innovation, this new framework even includes an enhancement for regulating the overlapping of dots of different channels.

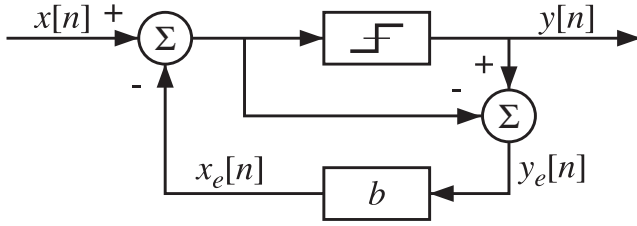


Figure 1: The error diffusion as first introduced by Floyd and Steinberg.

2. Generalized Error Diffusion

2.1. Monochrome

In error diffusion (Fig. 1), the output pixel $y[n]$ is determined by adjusting and thresholding the input pixel $x[n]$ such that

$$y[n] = \begin{cases} 1 & , \text{ if } (x[n] - x_e[n]) \geq 0 \\ 0 & , \text{ else} \end{cases} \quad (2)$$

where $x_e[n]$ is the diffused quantization error accumulated during previous iterations as

$$x_e[n] = \sum_{i=1}^M b_i \cdot y_e[n-i] \quad (3)$$

with $y_e[n] = y[n] - (x[n] - x_e[n])$ and $\sum_{i=1}^M b_i = 1$. Using vector notation, eqn. (3) becomes

$$x_e[n] = \mathbf{b}^T \mathbf{y}_e[n] \quad (4)$$

where $\mathbf{b} = [b_1, b_2, \dots, b_M]^T$ and $\mathbf{y}_e[n] = [y_e[n-1], y_e[n-2], \dots, y_e[n-M]]^T$.

In [8], Eschbach and Knox suggest modulating the threshold for quantization by the input image (Fig. 2) such that eqn. (2) becomes

$$y[n] = \begin{cases} 1 & , \text{ if } (x[n] - x_e[n] + kx[n]) \geq 0 \\ 0 & , \text{ else} \end{cases} \quad (5)$$

where k is a scalar quantity with increasing k leading to sharper edges in the halftoned image. By employing this threshold modulation, Eschbach and Knox eliminate the need for edge sharpening of the input image prior to halftoning.

Levien [4] makes his addition to error diffusion by including an output-dependent feedback term, Fig. 2, to eqn. (2) such that

$$y[n] = \begin{cases} 1 & , \text{ if } (x_a[n]) \geq 0 \\ 0 & , \text{ else} \end{cases} \quad (6)$$

where $x_a[n] = x[n] - x_e[n] + x_h[n]$ is the *accumulated* input pixel and $x_h[n]$ is the hysteresis or feedback term defined as

$$x_h[n] = h \sum_{i=1}^N a_i \cdot y[n-i] \quad (7)$$

with $\sum_{i=0}^N a_i = 1$ and h an arbitrary constant. Referred to as the *hysteresis constant*, h acts as a tuning parameter

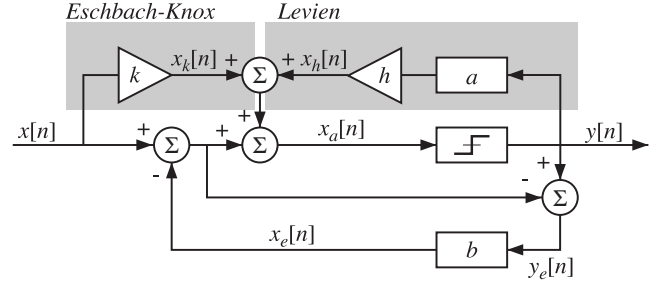


Figure 2: The error diffusion with output-dependent feedback as introduced by Levien along with the threshold modulation term proposed by Eschbach and Knox.

with larger h leading to coarser output textures [4] with h increasing ($h > 0$) or decreasing ($h < 0$) the likelihood of a minority pixel if the previous outputs were also minority pixels. Eqn. (7) can also be written in vector notation as

$$x_h[n] = h \mathbf{a}^T \mathbf{y}[n] \quad (8)$$

where $\mathbf{a} = [a_1, a_2, \dots, a_N]^T$ and $\mathbf{y}[n] = [y[n-1], y[n-2], \dots, y[n-N]]^T$. The calculation of the parameters $\mathbf{y}_e[n]$ and $x_e[n]$ remains unchanged in Levien's approach.

2.2. Color

Now consider the C -channel case where an output pixel is not the binary pixel $y[n]$ but the C -dimensional vector $\vec{y}[n]$ such that

$$\vec{y}[n] = \begin{bmatrix} y_1[n] \\ y_2[n] \\ \vdots \\ y_C[n] \end{bmatrix} \quad (9)$$

where $y_i[n]$ is the binary output pixel of color i . Assuming all C channels are halftoned independently, the binary output pixel $y_i[n]$ is determined as

$$y_i[n] = \begin{cases} 1 & , \text{ if } (x_{a_i}[n]) \geq 0 \\ 0 & , \text{ else} \end{cases} \quad (10)$$

where $x_{a_i}[n] = x_i[n] - x_{e_i}[n] + x_{h_i}[n]$ and $x_{e_i}[n]$ and $x_{h_i}[n]$ are the error and hysteresis terms respectively for the i^{th} color. The error term, being a vector, is calculated as

$$\vec{x}_e[n] = \mathbf{B} \mathbf{Y}_e[n] \quad (11)$$

where

$$\mathbf{B} = \begin{bmatrix} \mathbf{b}_1^T & 0 & \dots & 0 \\ 0 & \mathbf{b}_2^T & \dots & 0 \\ \vdots & \vdots & \ddots & \vdots \\ 0 & 0 & \dots & \mathbf{b}_C^T \end{bmatrix} \quad (12)$$

and

$$\mathbf{Y}_e[n] = \begin{bmatrix} y_{1_e}[n] \\ y_{2_e}[n] \\ \vdots \\ y_{C_e}[n] \end{bmatrix} \quad (13)$$

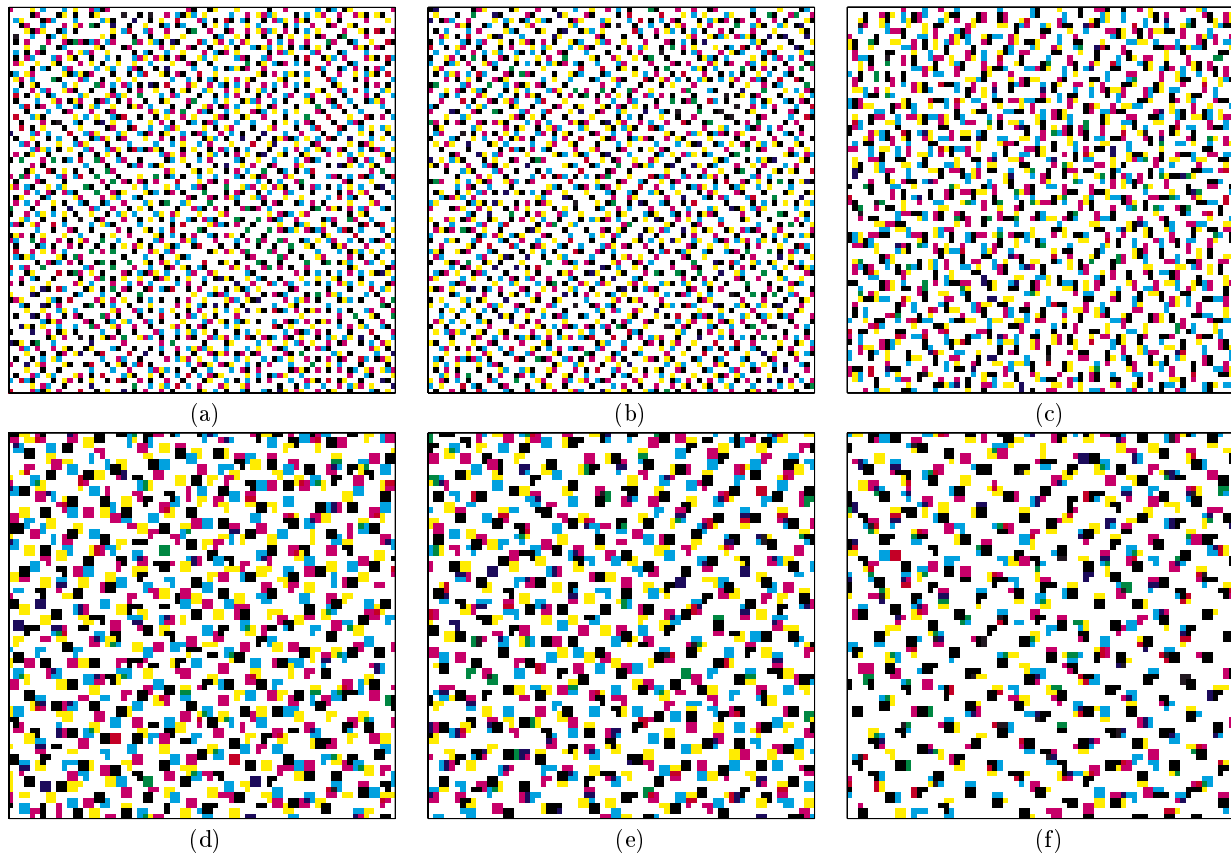


Figure 3: The resulting dither patterns created by generalized error diffusion where in (a) the parameters are set to perform Floyd's and Steinberg's original algorithm on each channel independently of the others, (b-c) each channel is halftoned independently using Levien's output-dependent feedback algorithm with (b) a small hysteresis constant $h = 0.5$ and (c) a medium constant $h = 1.0$. Dither patterns (d-f) are generated using output-dependent feedback with a large constant $h = 1.5$ with the interference matrix controlling dot overlap with (d) showing reduced overlap, (e) showing uncorrelated overlap, and (f) showing increased overlap.

such that \mathbf{b}_i are the filter weights regulating the diffusion of error in the i^{th} channel and $\mathbf{y}_{e_i}[n]$ is the vector $[y_{e_i}[n-1], y_{e_i}[n-2], \dots, y_{e_i}[n-N]]^T$ composed exclusively from errors in channel i such that $y_{e_i}[n] = y_i[n] - (x_i[n] - x_{e_i}[n])$. The hysteresis term $\bar{x}_h[n]$, also a vector, is calculated as

$$\bar{x}_h[n] = \mathbf{HAY}[n] \quad (14)$$

where

$$\mathbf{H} = \begin{bmatrix} h_1 & 0 & \dots & 0 \\ 0 & h_2 & \dots & 0 \\ \vdots & \vdots & \ddots & \vdots \\ 0 & 0 & \dots & h_C \end{bmatrix}, \quad (15)$$

$$\mathbf{A} = \begin{bmatrix} \mathbf{a}_1^T & 0 & \dots & 0 \\ 0 & \mathbf{a}_2^T & \dots & 0 \\ \vdots & \vdots & \ddots & \vdots \\ 0 & 0 & \dots & \mathbf{a}_C^T \end{bmatrix}, \quad (16)$$

and

$$\mathbf{Y}[n] = \begin{bmatrix} \mathbf{y}_1[n] \\ \mathbf{y}_2[n] \\ \vdots \\ \mathbf{y}_C[n] \end{bmatrix} \quad (17)$$

such that \mathbf{a}_i are the filter weights and h_i is the hysteresis constant that regulates the diffusion of feedback in the i^{th} channel.

Shown in Fig. 3(a) is the resulting CMYK dither patterns created by halftoning a 96×96 pixel color image of constant color value $\bar{x}[n] = [7/8, 7/8, 7/8, 7/8]^T$ using the Floyd-Steinberg [2] error filter weights with no hysteresis and no diffusion between colors. Shown in Fig. 3(b) is the resulting CMYK dither patterns created by implementing Levien's output-dependent feedback with a low hysteresis constant $h = 0.5$ and no diffusion between colors. With a low hysteresis constant, this scheme generates blue-noise patterns very similar to that generated using the Floyd-Steinberg filter weights. Fig. 3(c) shows Levien's output-dependent feedback with a medium hysteresis constant $h = 1.0$ where the patterns begin to exhibit clustering as the average size of a minority pixel cluster is 1.95 pixels.

To include Eschbach's and Knox's [8] threshold modulation into color halftoning, we redefine the accumulated input pixel as

$$\bar{x}_a[n] = \bar{x}[n] + \bar{x}_f[n] - \bar{x}_e[n] + \bar{x}_h[n] \quad (18)$$

where $\bar{x}_f[n]$ is the *feed-through* term defined as $\bar{x}_f[n] = \mathbf{K}\bar{x}[n]$ such that

$$\mathbf{K} = \begin{bmatrix} k_1 & 0 & \cdots & 0 \\ 0 & k_2 & \cdots & 0 \\ \vdots & \vdots & \ddots & \vdots \\ 0 & 0 & \cdots & k_C \end{bmatrix}. \quad (19)$$

We can extend our multi-channel scalar error diffusion algorithm defined by eqn. (11) to a vector algorithm by removing the constraint that quantization error must remain within its channel [9] by letting

$$\mathbf{B} = \begin{bmatrix} \mathbf{b}_{1,1}^T & \mathbf{b}_{1,2}^T & \cdots & \mathbf{b}_{1,C}^T \\ \mathbf{b}_{2,1}^T & \mathbf{b}_{2,2}^T & \cdots & \mathbf{b}_{2,C}^T \\ \vdots & \vdots & \ddots & \vdots \\ \mathbf{b}_{C,1}^T & \mathbf{b}_{C,2}^T & \cdots & \mathbf{b}_{C,C}^T \end{bmatrix} \quad (20)$$

where quantization error can now be diffused between channels through $\mathbf{b}_{i,j}$, the error filter weights which regulate the diffusion of error from channel j to channel i ; furthermore, eqn. (14) can be further generalized by setting

$$\mathbf{H} = \begin{bmatrix} h_{1,1} & h_{1,2} & \cdots & h_{1,C} \\ h_{2,1} & h_{2,2} & \cdots & h_{2,C} \\ \vdots & \vdots & \ddots & \vdots \\ h_{C,1} & h_{C,2} & \cdots & h_{C,C} \end{bmatrix} \quad (21)$$

and

$$\mathbf{A} = \begin{bmatrix} \mathbf{a}_{1,1}^T & \mathbf{a}_{1,2}^T & \cdots & \mathbf{a}_{1,C}^T \\ \mathbf{a}_{2,1}^T & \mathbf{a}_{2,2}^T & \cdots & \mathbf{a}_{2,C}^T \\ \vdots & \vdots & \ddots & \vdots \\ \mathbf{a}_{C,1}^T & \mathbf{a}_{C,2}^T & \cdots & \mathbf{a}_{C,C}^T \end{bmatrix} \quad (22)$$

where the previous outputs of channel j can impact all other channels where $h_{i,j} \neq 0$ for $i \neq j$ as $\mathbf{a}_{i,j}$ and $h_{i,j}$ regulate the diffusion of feedback from channel j to i . We can also allow inputs of different channels to impact other channels by setting

$$\mathbf{K} = \begin{bmatrix} k_{1,1} & k_{1,2} & \cdots & k_{1,C} \\ k_{2,1} & k_{2,2} & \cdots & k_{2,C} \\ \vdots & \vdots & \ddots & \vdots \\ k_{C,1} & k_{C,2} & \cdots & k_{C,C} \end{bmatrix}. \quad (23)$$

Before concluding this section, we first define the thresholding function $T(\cdot)$ as

$$T(\bar{x}_a[n]) = \begin{cases} 1 & , \text{ if } (\bar{x}_a[n]) \geq 0 \\ 0 & , \text{ else} \end{cases} \quad (24)$$

such that $\bar{y}[n] = T(\bar{x}_a[n])$. Then the $C \times C$ interference matrix \mathbf{S} is added to eqn. (24) as

$$\bar{y}[n] = T(\mathbf{S}\bar{x}_a[n]) \quad (25)$$

such that $S_{i,j}$ is the influence on the thresholding function of color i by the accumulated input of color j . The effect of

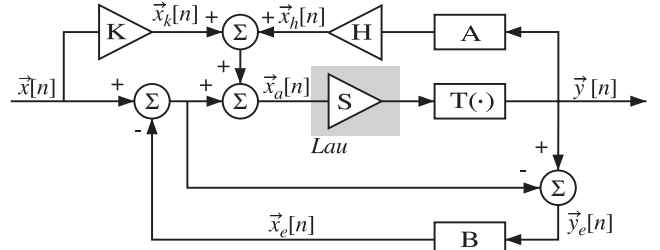


Figure 4: The generalized error diffusion algorithm.

$S_{i,j}$ is to increase ($S_{i,j} > 0$) or decrease ($S_{i,j} < 0$) the likelihood of a minority pixel at $y_i[n]$ based on the likelihood of a minority pixel at $y_j[n]$. Finally, we can summarize error diffusion by the *generalized error diffusion equation*

$$\bar{y}[n] = T(\mathbf{S}(\mathbf{K}\bar{x}[n] - \mathbf{B}\bar{y}_e[n] + \mathbf{H}\bar{A}\bar{y}[n])), \quad (26)$$

Fig. 4. Note that in eqn. (26), we have absorbed the $\bar{x}[n]$ term into $\mathbf{K}\bar{x}[n]$.

The dither patterns of Fig. 3(d-f) illustrate the effects of \mathbf{S} , the interference matrix, with Fig. 3(d) showing the case where \mathbf{S} is the matrix defined by $S_{i,j} = 1$ for $i = j$ and $S_{i,j} = -0.2$ for $i \neq j$. In all instances where $S_{i,j} < 0$, \mathbf{S} has the effect of reducing the superposition of minority pixels of different colors with lesser $S_{i,j}$ leading to lesser overlap. That is, given that a cyan pixel is very likely to be printed, minority pixels for magenta, yellow and black are less likely to be printed at that same pixel location. For comparison, Fig. 3(e) shows the case where \mathbf{S} is the identity matrix (no interference) and Fig. 3(f) shows the case where \mathbf{S} is the matrix defined by $S_{i,j} = 1$ for $i = j$ and $S_{i,j} = +0.2$ for $i \neq j$. Here in Fig. 3(f), the effect of \mathbf{S} is to increase the superposition of minority pixels such that a minority pixel of color i with a high likelihood of being printed making a minority pixel of any color j more likely.

3. Spatial Analysis

As a means of characterizing the spatial distribution of pixels in the dither patterns of Fig. 3, we can use the point process statistics introduced to halftoning by Lau *et al* [5], but in the case of a color halftone, the monochrome model I_g must be revised as a dither pattern is now composed of C colors with the halftone pattern I_g now composed of the monochrome binary dither patterns $I_{g_1}, I_{g_2}, \dots, I_{g_C}$ where g_i is the gray level of pattern I_{g_i} and ϕ_i is the corresponding point process. Extending Lau *et al*'s [5] monochrome pair correlation to color halftoning, the pair correlation between colors g_i and g_j follows as

$$\mathcal{R}_{i,j}(r) = \frac{\mathbf{E}\{\phi_{g_i}(R_m(r)) \mid \phi_{g_j}[m] = 1\}}{\mathbf{E}\{\phi_{g_i}(R_m(r))\}}, \quad (27)$$

the ratio of the expected number of minority pixels of color g_i located in the ring $R_m(r) = \{nr < |n - m| \leq r + dr\}$ under the condition that $\phi_{g_j}[m]$ is a minority pixel to the unconditional expected number of minority pixels with color g_i located in $R_m(r)$.

For a statistical analysis of the dither patterns of Fig. 3, Fig. 5(top) shows the pair correlation in Fig. 3(a) between colors cyan versus cyan ($\mathcal{R}_{c,c}(r)$), cyan versus magenta ($\mathcal{R}_{c,m}(r)$), cyan versus yellow ($\mathcal{R}_{c,y}(r)$) and cyan versus black ($\mathcal{R}_{c,k}(r)$). The small diamonds placed along the

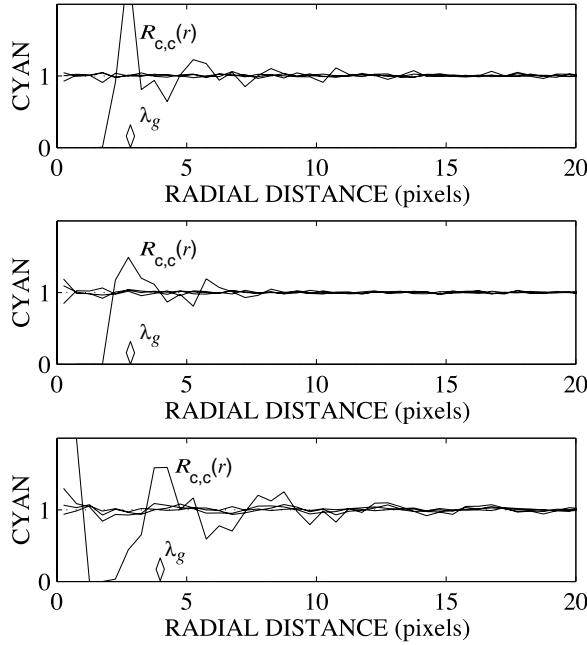


Figure 5: The pair correlations for CMYK halftone patterns with no diffusion between colors using (top) Floyd-Steinberg error diffusion weights and no hysteresis, (middle) Levien diffusion with small hysteresis constant ($h = 0.5$) and (bottom) Levien diffusion with medium hysteresis constant ($h = 1.0$).

horizontal axis indicate the principle wavelengths and possible cluster radii for $\mathcal{R}_{c,c}(r)$. As would be expected for a monochrome image, the pair correlation $\mathcal{R}_{c,c}(r)$ exhibits blue-noise characteristics as the pair correlation shows: (i) $\mathcal{R}_{c,c}(r) < 1$ for r near zero, (ii) a frequent occurrence of the inter-point distance λ_g and (iii) a decreasing influence with increasing r . Having no diffusion between colors and zero interference ($\mathbf{S} = \mathbf{I}$, the identity matrix), the pair correlations between channels are predominantly flat as minority pixels of color i have no influence on minority pixels of color j .

Shown in Fig. 5(center and right) are the resulting cyan pair correlations to Fig. 3(b and c) where Levien's error diffusion scheme has been implemented. With a low hysteresis constant (Fig. 3(b)), this scheme generates pair correlations (Fig. 5(middle)) very similar to those of Floyd and Steinberg. Using a medium hysteresis constant $h = 1.0$ where the patterns begin to exhibit clustering, the pair correlation exhibits stronger green-noise characteristics as each plot shows: (i) clustering as indicated by $\mathcal{R}_{i,i}(r) \geq 1$ for $r \leq r_c$ ($r_c = 0.79$), (ii) a frequent occurrence of the inter-cluster distance $\lambda_g = 3.95$ and (iii) a decreasing influence with increasing r . Without interference between colors, the pair correlations between colors remain predominantly flat for all r .

In Fig. 6, the behavior to increase or decrease ink overlap through \mathbf{S} is will illustrated in the pair correlation. In the case of Fig. 6(top) (Fig. 3(d)), the decrease in ink overlap is evident where $\mathcal{R}_{i,j} < 1$ for $\mathcal{R}_{i,i} > 1$. In Fig. 6(middle) (Fig. 3(e)), \mathbf{S} creates no interference and illustrates this as $\mathcal{R}_{i,j} = 1$ regardless of $\mathcal{R}_{i,i}$. By increasing overlap in Fig. 3(f), \mathbf{S} creates in Fig. 6(bottom) pair correlations where $\mathcal{R}_{i,j} > 1$ for $\mathcal{R}_{i,i} > 1$.

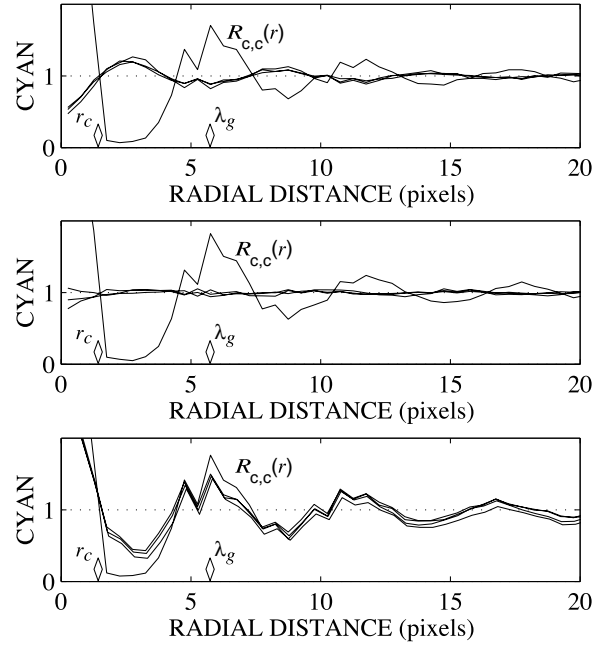


Figure 6: The pair correlations for CMYK halftone patterns using Levien diffusion with high hysteresis constant ($h = 1.5$) with (top) a negative interference term ($S_{i \neq j} = -0.2$), (middle) no interference term ($S_{i \neq j} = 0$) and (bottom) a positive interference term ($S_{i \neq j} = +0.2$).

4. Conclusions

In this paper, I introduced a general framework for error diffusion in multi-channel environments. This new framework is applicable to both scalar and vector error diffusion, but while numerous enhancements have been incorporated into this new algorithm, I have only demonstrated two: Levien's output-dependent feedback and a novel enhancement, the interference matrix. Feedback's contribution is to allow clustering, making generalized error diffusion a plausible halftoning scheme in laser printers, which typically cannot print the isolated dots of blue-noise.

The interference matrix allows for the control of ink overlap between colors. Controlling this overlap is useful when you consider paper coverage that by minimizing the overlap, you are maximizing paper coverage. In turn, you are maximizing the spatial frequency of dots, thereby, making the halftone pattern less visible. But any gains made through the interference matrix quickly diminish with even slight mis-registration between screens.

With regards to the other enhancements, my comments are, for now, conjecture. Consider Eschbach's and Knox's threshold modulation scheme. In generalized error diffusion, do not think of \mathbf{K} as a scalar diagonal matrix that sharpens each channel independently. Instead, consider \mathbf{K} as representing a mapping of the CMYK color space to a luminance value. In this instance, \bar{x}_f will sharpen each color's dither pattern according to the image's luminance channel.

Now while diffusion of error between channels is shown by Akarun *et al* [9] to improve results over strict scalar error diffusion, diffusion of feedback between channels is still untested, but it seems reasonable that properly selected hysteresis weights could further separate the dots of different colors. Where the interference matrix only moves a dot to the next available slot, \bar{x}_h could move dots multi-

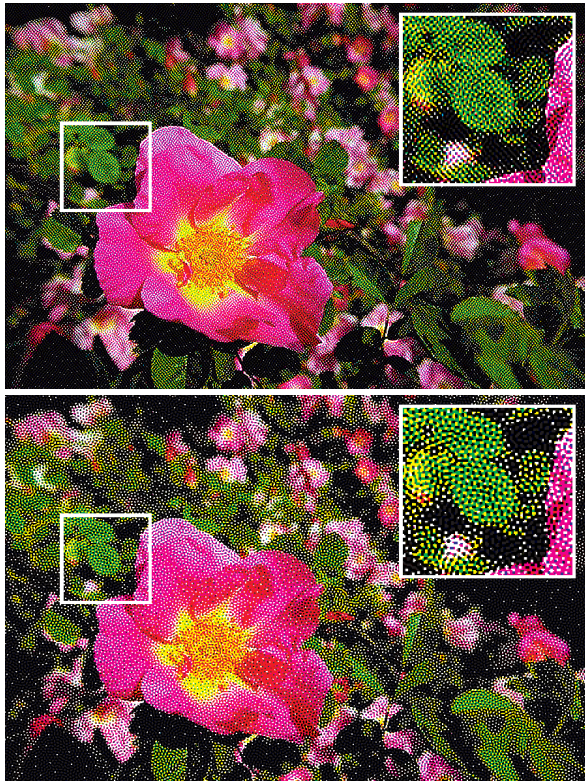


Figure 7: CMYK images halftoned using (top) generalized error diffusion with output-dependent feedback where the interference matrix is minimizing overlap between colors and (bottom) multi-channel green-noise masks constructed to also minimize the overlap between colors.

ple pixels apart. This may relieve the strict tolerances on screen registration when each channel is so closely correlated.

Future work with generalized error diffusion will be sure to answer these questions. In closing, I wish to point out that while generalized error diffusion may be too computationally complex for a commercial application, insight gained using this new framework may lead to advancements in less complex halftoning algorithms. I note Fig. 7 where the reduction in overlap using the interference matrix (Fig. 7(top)) is achieved using multi-channel green-noise masks [10] (Fig. 7(bottom)).

5. Acknowledgment

This work has been sponsored, in part, by Lexmark International Inc, Lexington KY USA.

References

[1] R. A. Ulichney, "The void-and-cluster method for dither array generation," in *Proceedings SPIE, Human Vision, Visual Processing, Digital Displays IV* (B. E. Rogowitz and J. P. Allebach, eds.), vol. 1913, pp. 332-343, Feb. 1993.

- [2] R. W. Floyd and L. Steinberg, "An adaptive algorithm for spatial gray-scale," *Proceedings Society Information Display*, vol. 17, no. 2, pp. 75-78, 1976.
- [3] R. A. Ulichney, "Dithering with blue noise," *Proceedings of the IEEE*, vol. 76, pp. 56-79, Jan. 1988.
- [4] R. Levien, "Output dependant feedback in error diffusion halftoning," in *IS&T's Eighth International Congress on Advances in Non-Impact Printing Technologies*, (Williamsburg, Virginia, USA), pp. 280-282, October 25-30 1992.
- [5] D. L. Lau, G. R. Arce, and N. C. Gallagher, "Green-noise digital halftoning," *Proceedings of the IEEE*, vol. 86, pp. 2424-2444, Dec. 1998.
- [6] B. E. Cooper and D. L. Lau, "An evaluation of green-noise masks for electrophotographic halftoning," in *Proceedings of the IS&T's and SPIE's Electronic Imaging*, (San Jose, California, USA), January 22-28 2000.
- [7] K. T. Knox, "The evolution of error diffusion," *Journal of Electronic Imaging*, vol. 8, pp. 422-429, Oct. 1999.
- [8] R. Eschbach and K. T. Knox, "Error-diffusion algorithm with edge enhancement," *Journal of the Optical Society of America*, vol. 8, pp. 1844-1850, December 1991.
- [9] L. Akarun, Y. Yardimci, and A. E. Cetin, "Adaptive methods for dithering color images," *IEEE Transactions on Image Processing*, vol. 6, no. 7, pp. 950-955, 1997.
- [10] D. L. Lau, G. R. Arce, and N. C. Gallagher, "Digital color halftoning via generalized error-diffusion and vector green-noise masks," *IEEE Transactions on Image Processing*, Submitted February 1999.

6. Biography

Dr. Daniel L. Lau received his B.S. in Electrical Engineering from Purdue University, West Lafayette with highest distinction in 1995 and then his Ph. D. degree in Electrical Engineering at the University of Delaware in 1999. Daniel spent a year signal and image processing at the Lawrence Livermore National Laboratory in California and is currently a visiting assistant professor at the University of Delaware. His published works in halftoning include an article in the December 1998 issue of the *Proceedings of the IEEE*.